Bearing Fault Identification using Watershed-Based Thresholding Method

H. Fandiño-Toro, O. Cardona-Morales, J. Garcia-Alvarez and G. Castellanos-Dominguez

Abstract In this work, a novel thresholding method is proposed to improve the accuracy in segmentation process on thermal images. Characteristics of the thermal distribution around convex Regions of Interest (ROI) are the core of this method, used as input markers for a segmentation process based on watershed transform. This method based on data variability reduces the classification error by about 10 % and reduces the number of features by about 80 % from the set of 360 elements. Moreover, the proposed method provides some tracks for fault localization, demonstrated for a bearing unbalance test rig.

Keywords Fault identification · Thresholding · Region of interest · Thermal images

1 Introduction

Bearing faults, like motor shaft misalignment, cause damages on rotating machine parts such as couplings, bearings, engine components and loads, among others [1]. Therefore, the main goal of machine maintenance is to avoid the unexpected

H. Fandiño-Toro (✉) · O. Cardona-Morales · J. Garcia-Alvarez · G. Castellanos-Dominguez
Signal Processing and Recognition Group, Universidad Nacional de Colombia,
Km 9 way to airport, Campus la Nubia, Manizales, Republic of Colombia
e-mail: hfandinot@unal.edu.co

O. Cardona-Morales
e-mail: ocardonam@unal.edu.co

J. Garcia-Alvarez
e-mail: jcgarciaa@unal.edu.co

G. Castellanos-Dominguez
e-mail: cgcastellanosd@unal.edu.co

G. Dalpiaz et al. (eds.), *Advances in Condition Monitoring of Machinery in Non-Stationary Operations*, Lecture Notes in Mechanical Engineering,
DOI: 10.1007/978-3-642-39348-8_11,

machine damages, using two maintenance strategies: corrective and preventive. For the former one, the machine operator repairs or replaces the damaged part as soon as the fault is present. In addition, the latter one suggests the frequent inspection on the machine, assessing the machine part deterioration degree. Hence, an adequate preventive maintenance would be accomplished by providing adequate information of some Region of Interest (ROI) on thermal image, where the hot spots would be located. However, due to the characteristics of thermal images, conventional methods of ROI segmentation are not adequate [2], giving this segmentation to be manually accomplished by the human expert.

In this work, the proposed multi-level thresholding method improves the ROI segmentation method for thermal images, thus giving local information for machine fault identification. Based on the local variability of the pixel distribution of thermal images, the method gives the following features: first, the threshold adjustment is invariant of the statistical distribution model estimated from the image; secondly, the thresholding method fits with segmentation techniques for images exhibiting variability around local maximal values.

2 Proposed Thresholding Method

Variations measured on thermal image are limited by the geometry of each machine part. Thus, thermal changes occur at low contrast areas, bounded by smooth edges. Therefore, ROI segmentation is adequate to characterize several machine parts, depending on the thermal pattern exhibited in operation. In this case, the Watershed Transform is a commonly segmentation technique, where the topological gradient image generates borders, namely watershed lines, which define the contour of a segmented object on the image.

Proposed method consists on a modified iterative extraction of disjoint intervals, based on the pixel distribution in the image, generating the quantized image with the weighted average of the values belonging each interval, and then assigned to represent each element of image [3]: noting $\boldsymbol{X}$ as the original thermal image, k as a threshold parameter, and $[T_1, T_2]$ as the interval calculated for some iteration, following algorithm describes the proposed method:

Step 1. The first interval (at the iteration $n = 0$) is defined as $[T_a(0), T_b(0)] = [\mathrm{a, b}]$, where $a = min\ (\boldsymbol{X})$ and $b = max\ (\boldsymbol{X})$;

Step 2. For each interval $[T_a(n), T_b(n)]$ at the iteration n, the weighted mean μ and standard deviation are calculated a [j]

Step 3. Thresholds for the next iteration n + 1 are calculated as: $T_a(n+1) = \mu - k\sigma$ and $T_b(n+1) = \lfloor \mu + k\sigma \rfloor$, where $\lfloor . \rfloor$ denotes floor operation;

Step 4. A new interval is created as:
$[T_a(n+1),\ T_b(n+1)] = [T_a(n+1)+1,\ T_b(n+1)-1]$, the increment/decrement of the interval values by 1 avoids interval overlapping;

Step 5. Pixel values belonging inside remaining intervals $T_{Ra} = [T_a(n), T_a(n+1)]$ and $T_{Rb} = [T_b(n), T_b(n+1)]$ are represented in quantized image with the respective values $\mu(T_{Ra})$ and $\mu(T_{Rb})$;

Step 6. If $T_a(n) - T_b(n) \geq 2$, update $n = n+1$, then go to Step 2.

Hence, the proposed method suggests that those pixel sets containing a high-grade of variability belong to a convex ROI. Moreover, parameter k is unknown. An inadequate choice of this parameter can lead to inaccurate quantization of the image, therefore a value of k is empirically estimated to get several intervals related with convex *ROIs*.

Another problem concerns with objects not belonging to the fault identification process, like cables and sensors, appearing as segmented *ROIs*. To address this problem, the segmentation process uses a region–based masking, eliminating those connected regions being less than z pixels in the image. This assumes that the objects inside the ROI of size less than z pixels are not relevant to the identification process. Thus, following algorithm describes the segmentation process:

Step 1. The proposed thresholding algorithm processes the thermal image, giving quantized masks. The first high–valued quantized interval corresponds to *ROI*–candidate areas, generating the binarized image by assigning ones at the *ROI*–candidate areas, and zero otherwise.

Step 2. Watershed Transform segments the ROI on thermal image, using as local minimal those values at the center inside of the watershed lines. It gives a number of watershed regions.

Step 3. Comparison between statistical mode of the values of each watershed region, and the statistical mode of same region in binarized image. If the latter value is equal to zero, the watershed region is discarded. Thus, labeling of the remaining watershed regions is $ROIm$, $m = 1, \ldots, M$, where M is the number of remaining *ROIs*.

3 Feature Extraction for Fault Identification

If the thermal camera detects some isotropic heat propagation, then an isotropic gradient operator (like Gaussian) is capable to identify a possible fault, by estimating the probability that a pixel belongs to a relevant *ROI* [4]. However, faults can appear as anisotropic contour regions; then, an anisotropic operator would obtain information about the value and direction in which heat spreads. In this case, the usage of Sobel and Prewitt gradient operators allow detecting changes of heat propagation magnitude and direction in image for fault identification purposes.

Thus, the gradient operators T_x and T_y are calculated for the directions x and y of the thermal image $\boldsymbol{X}$, respectively, as

$$T_x = \begin{bmatrix} -1 & 0 & +1 \\ -2 & 0 & +2 \\ -1 & 0 & +1 \end{bmatrix}; \quad T_y = \begin{bmatrix} -1 & -2 & -1 \\ 0 & 0 & 0 \\ +1 & +2 & +1 \end{bmatrix} \tag{1}$$

$$T_x = \begin{bmatrix} -1 & 0 & +1 \\ -1 & 0 & +1 \\ -1 & 0 & +1 \end{bmatrix}; \quad T_y = \begin{bmatrix} -1 & -1 & -1 \\ 0 & 0 & 0 \\ +1 & +1 & +1 \end{bmatrix} \tag{2}$$

where Eqs. (1) and (2) refer to the Sobel and Prewitt operators, respectively. Thus, the convolution between image and either vertical T_x or horizontal T_y gradient operator gives the gradient vectors $G_x = T_x * \boldsymbol{X}$ and $G_y = T_y * \boldsymbol{X}$, respectively. Finally, Eq. (3) extracts the gradient direction feature α at each pixel position (x, y) as:

$$\alpha(x, y) = \tan^{-1}\left(\frac{G_y}{G_x}\right) \tag{3}$$

4 Experimental Set-Up

Evaluation of the proposed method consists on its implementation on a rotating machine fault identification system. Specifically, the method belongs to the ROI segmentation process on the thermal image used for fault identification. The following steps are part of the evaluation process: (1) processing of acquired thermal image by the proposed method, giving a quantized image under a selected parameter k; (2) mapping of the quantized image, giving the watershed lines within the *ROI* segmentation algorithm; (3) gradient feature extraction from segmented *ROIs*; (4) calculation of classification error rate for different machine conditions, using parameter k as variable and gradient values as inputs.

4.1 Test Rig and Image Database

Figure 1 shows the testing rotating machine of the fault identification system, consisting of a three-phase induction motor, with a rigid coupling between its shaft and another shaft containing 2 drilling wheels. Insertion of weights of arbitrary mass in one of these wheels induces the following two unbalance types: the first one, by inserting weights in the drilling wheel closer to 12 cm from the dock, being labeled as *First Wheel Unbalance* (FWU); the second one, called *Second Wheel Unbalance* (SWU), by inserting weights into the farther bearing at 43.5 cm

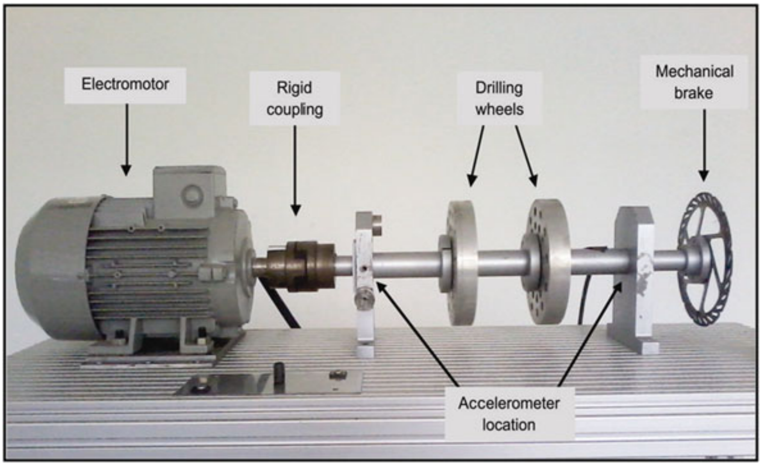

Fig. 1 Test rig image

from the coupling. Machine operation recording lasts 2 h since its startup. Thus, there is an observation for each different operating condition: Normal, FWU and SWU.

Thermal image is the result of the decomposition of recorded video frames into a YUV-space color image sequence. At a video recording rate of 1 frame per 60 s, and noting that the first and second hour of machine operation is an adequate observation time (when the motor achieves a stable temperature), the total number of recorded images per observation is then 60. Moreover, each required image comes from the Y intensity plane of each element of YUV-space sequence, since this plane is a projection of the thermal chroma values. Table 1 shows other video recording parameters.

By observation of the operation conditions, a preliminary segmentation of a ROI corresponding to the first and second bearing aims to improve the fault identification process [5], because thermal variations in this *ROI* are directly related to the mechanical effects due to unbalance. Thus, the *ROI* labeled as *ROI*12 in Fig. 2 is the database image, used for the segmentation algorithm.

4.2 Thresholding and Segmentation

The k-parameter adjustment assures a finite number of disjoint intervals related with convex *ROIs*. So, at a determined value k, the high–valued intervals keep the maximal information of thermal distribution. In this case, values of $k = 1, 2, 3$ are previously assigned. Besides, a region–based masking is implemented after the thresholding process to prevent including of non-relevant objects for the identification process, such as the sensor and cable objects placed along the machine.

Table 1 Video camera specifications

Camera parameters (FLIR A320)	Emissivity	0.82
	Reflected temperature	20 °C
	Distance between camera and test rig	1.5 m
	Relative humidity	50 %
	Ambient temperature	20 °C
	Thermal scale	10–50 °C
	Frame size	640 × 480 pixels
Video acquisition parameters	Video format	MPEG-2

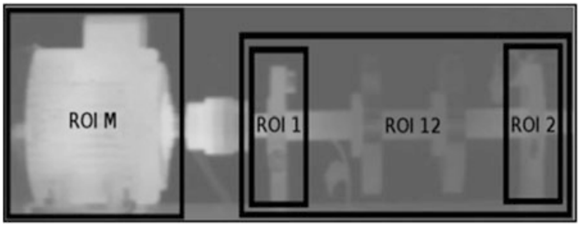

Fig. 2 Some preliminary ROIs

By observation of non-relevant objects in image, an assumed ROI size threshold is z = 200 pixels. This value would vary for another experiments and test rigs. The coordinates of pixels belonging selected ROIs are part of the data required for the feature extraction process.

4.3 Feature Extraction and Classification Error Rate

The Edge Direction Histogram (EDH), proposed in (6), determines the relevant phase values α used for fault identification, for each segmented ROI M: (1) Eq. (3) extracts the gradient direction $\alpha$for each point, using either Prewitt or Sobel operator; (2) rounding of each direction, up to the nearest integer value, gives the direction vector $\vec{p} = \{\alpha(x, y)\} \in N$, for each coordinate $(x, y) \in N$; (3) Principal Component Analysis (PCA),based on histogram of direction vector $\vec{p}$, gives the-relevance weight for each direction.

After sorting of the relevant directions, evaluation of classification performance requires 10 cross-validation trials (70 % training and 30 % validation images, sorted randomly), by comparing the classification error between trials using all directions and trials using the most relevant directions. Noting that location is the main characteristic for considered fault conditions (FWU and SWU), the evaluation for each selected ROI M would give a track for not only fault identification, but also fault localization, defined as Localized Fault Identification (*LFI*) [2]. The number of relevant directions α are found when the classification error value is less than 10 %.

5 Results

5.1 Thresholding and Segmentation

Figure 3 shows the mean and standard deviation of quantized values for the three most high–valued intervals, for each considered operation condition, calculated by proposed thresholding method, using $k = 1, 2, 3$. In this case, the optimal value k' is found at the maximal distance between the mean value of first and second interval. This condition implies that the method provides adequate thresholds for the segmentation process, allowing this an accurate ROI segmentation [6]. As result, the selected value is $k' = 1$.

Moreover, the mean number of iterations achieved in Table 2 measures the proposed threshold method performance, for considered parameter values $k' = 1, 2, 3$. In this case, the lower number of iterations is found at $k = k' = 1$, for the three considered conditions.

Figure 4 shows an example of the calculated intervals per iteration, using the proposed thresholding method at k' In this case, the test image corresponds to the 3600 s interval, under FWU condition; thresholding process stops at 4 iterations, giving a total of 8 intervals. For the sake of illustration, interval labels are by magnitude level order. As result, the interval number 1 gathers the highest thermal values, related with high variability.

Thereafter, results on segmentation process (Fig. 5) describes the following: (1) quantization of thermal database image, by the proposed thresholding method using the parameter k', gives the quantized image of Fig. 5a, where the highest

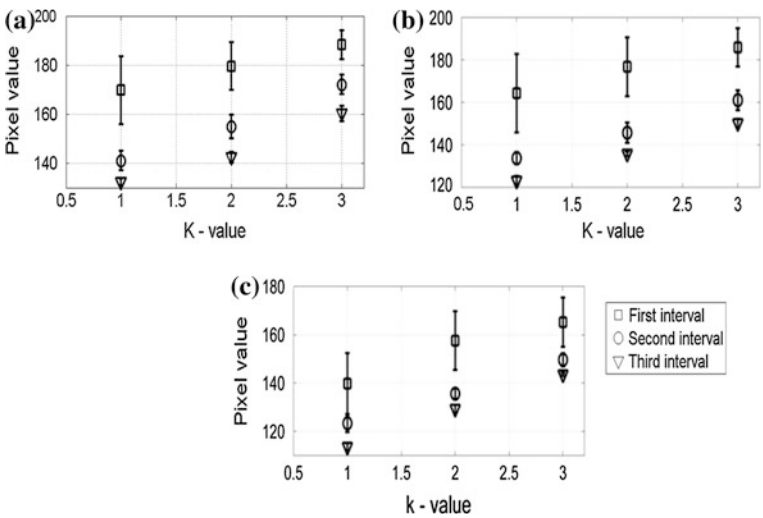

Fig. 3 Intervals with higher pixels for the considered operating conditions. **a** FWU. **b** SWU. **c** Normal

Table 2 Thresholing iterations for different k values

Operating condition	K value		
	1	2	3
FWU	4	7	13
SWU	4	7	17
Normal	4	7	18

interval (in white) fits with convex ROIs; (2) the masks belonging to the first interval composes the binarized image shown in Fig. 5b; (3) the watershed transform segments the thermal image, using region borders as watershed lines shown in Fig. 5c; (4) the region–based masking eliminates regions not belonging to identification processes; in this case, the regions belonging to an accelerometer sensor and a power cable disappear from segmented image (Fig. 5d); (5) finally, the labels for each segmented ROI masks appears in Fig. 5e as $ROIm, m = 1, \ldots, 5$.

5.2 Feature Extraction and Classification Error Rate

Direction feature extraction, for each labeled $ROIm$ and for the database image $ROI12$, gives correspondent sample vectors required as inputs of classification process. Figure 6 shows the results on the comparison between classification error of each $ROIm$ and error of $ROI12$. For the Prewitt operator, $ROI3$, $ROI4$ and $ROI5$ achieve an error lower than $ROI12$, requiring less number of relevant α values. Moreover, the classification error obtains less than 10 % using around of 8 orientations at $ROI3$, 4 orientations at $ROI4$, and 10 orientations at $ROI5$. In the case of the Sobel Operator, also $ROI3$, $ROI4$, and $ROI5$ achieve an error lower than $ROI12$, requiring less number of relevant α values, giving classification errors less

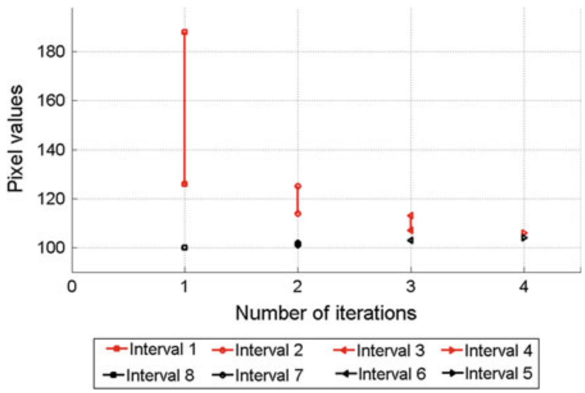

Fig. 4 Resulting intervals after thresholding process using proposed method k = 1

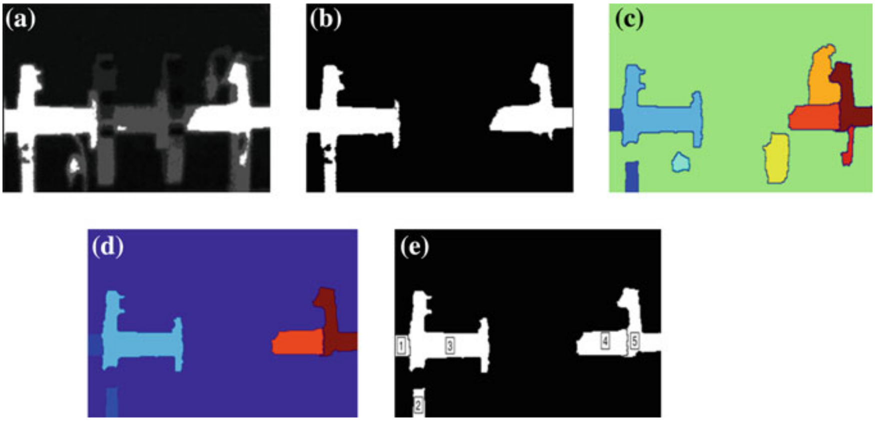

Fig. 5 ROI12 thermal image segmentation process. **a** Quantized image. **b** Mask for ROIs. **c** Preliminary Watershed segmentation. **d** Masks for ROIs after false object extraction. **e** Labeled ROIs after segmentation

than 10 % using around of 8 orientations at $ROI3$, 3 orientations at $ROI4$, and 8 orientations at $ROI5$.

6 Discussion

Given results of Fig. 4 indicate that the proposed thresholding method is adequate for fault identification, by observing the calculated intervals for different operation conditions. For example, using adjust parameter $k = 1$, a thermal variation between 120 and 140 of the quantized value of the first interval means that the machine is in Normal condition, whereas a thermal variation above 140 of the quantized value, at the same interval, would be identified as a fault.

From given results of Fig. 5, the proposed method gathers the most measured variations into one interval, using the fewest number of iterations at $k = 1$. In this case, the first interval achieves the most variable values, at the first iteration. Since the thresholding process is not enough for adequate fault localization, results of Fig. 5a and b give a relationship between the most variable interval and convex ROI, relating both thresholding and segmentation processes. In this case, the highest interval fits with convex ROIs of greater value variability. Using the given results of Fig. 5c–e, the proposed method helps to the watershed segmentation process with the following: firstly, avoiding the over–segmentation; secondly, eliminating those regions not belonging for the identification process.

Results given from Fig. 6 show that the number of relevant elements of the direction gradient feature α is around 10. Although the minimal number of relevant directions correspond to $ROI4$ using the Sobel operator, the $ROI4$ and $ROI5$ can

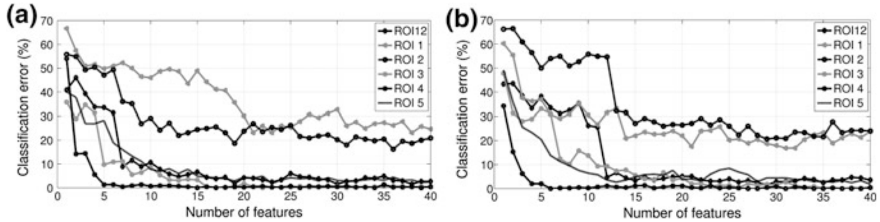

Fig. 6 Classification error using gradient features from segmented ROIs. **a** Prewitt operator. **b** Sobel operator

achieve a less number of relevant directions α, using the Prewitt operator. Therefore, selection of latter operator gives an adequate feature extraction process. Hence, the proposed thresholding method, with parameter $\kappa = 1$, gives segmented *ROIs* reducing the bearing fault classification error by about 10 % and reducing the number of relevant features by about 80 %, in comparison with the image $ROI12$. Finally, using results shown in Fig. 6, for both operators, $ROI4$ would be the key region for fault localization.

7 Conclusion

In this work, a proposed multi–level thresholding method improves the segmentation process of convex Regions of interest (ROI) for image–based fault identification and location systems.

Method evaluation uses a bearing fault identification system, requiring as input database a thermal image acquired on related test rig, the watershed transform as segmentation process, and the orientation gradientα as fault identification feature. Results provide the following highlights: (1) the method provides an adequate measure for fault identification, calculating an interval related with convex ROIs, being candidates to enclose a fault zone; (2) reduction of feature elements is suggested, to increase the fault classification rate, giving the Prewitt operator as adequate for feature extraction; (3) for this test rig, segmented $ROI3, ROI4$ and $ROI5$ are candidate regions for fault location.

Following works will be under consideration: firstly, a comparison between the quantized value of the proposed thresholding method and other measures, such as the statistical measures proposed in [7] for fault identification systems using thermal images; secondly, the usage of another feature, like Local Binary Patterns, to improve the accuracy of fault identification and localization system; finally, the use of method on other test rigs related with machine faults, acquiring more information about the fault phenomena.

Acknowledgments The authors acknowledge to Colciencias and the Universidad Nacional de Colombia for the financial support of the research projects "*Sistema autónomo de monitoreo de vibraciones para diagnóstico de fallas no estacionarias*" (with code 1101-521-28792).

References

1. Hoppler R, Errath R (2007) Motor bearings, not must a piece of metal. In: Proceedings of IEEE cement industry technical conference record, pp 214–233
2. Fandiño-Toro H, García-Álvarez J, Castellanos-Domínguez G (2011) Performance evaluation of measures for the thermographic detection of motor faults by mass unbalance. In: Proceedings of the international conference surveillance 6
3. Arora S, Acharya J, Verma A, Panigrahi P (2008) Multilevel thresholding for image segmentation through a fast statistical recursive algorithm. Pattern Recogn Lett 29(2):119–125
4. Ortiz-Jaramillo B, Fandiño-Toro H, Benitez-Restrepo H, Orjuela-Vargas S, Castellanos-Domínguez G, Philips W (2012) Multi-resolution analysis for region of interest extraction in thermographic, non-destructive evaluation. In: Proc SPIE 8295:82951
5. Widodo A, Satrijo D, Huda M, Lim G, Yang B (2011) Application of self organizing map for intelligent machinefault diagnostics based on infrared thermography images. In: Proceedings of IEEE 2011 sixth international conference on bio-inspired computing: theories and applications (BIC-TA), pp 123–128
6. Gao X, Xiao B, Tao D, Li X (2008) Image categorization: graph edit distance + edge direction histogram. Pattern Recogn 41(10):3179–3191
7. Younus A, Yang B (2009) Wavelet coefficient of thermal image analysis for machine fault diagnosis. In: Proceedings of the international conference on mechanical engineering, ICME09, pp 1–6